Multispectral, High-Resolution Satellite Observations of Plumes on Top of Convective Storms

VINCENZO LEVIZZANI

Institute FISBAT–CNR, Bologna, Italy

MARTIN SETVÁK

Satellite and Radar Department, Czech Hydrometeorological Institute, Prague, Czech Republic

(Manuscript received 1 November 1994, in final form 18 August 1995)

ABSTRACT

Multispectral, high-resolution imagery from the Advanced Very High Resolution Radiometer of NOAA polar orbiting satellites is used to analyze the cloud-top structure of convective storms that develop a cirrus feature above the anvil, referred to as a *plume*, whose origin remains unclear. Images from the radiometer's channels 2, 3, and 4 and a combination of any two of these suggest a relationship between the emergence of such plumes and a source of small ice particles (diameter around 3.7 μm, channel 3 wavelength) at the cloud top. Unique observations of deep convective storms over Europe are presented and discussed. The paper does not provide an exhaustive explanation of the phenomenon but contributes original material to the study of convective storm cloud-top structure, which is far from being completely described.

1. Introduction

Significant cloud-top features, associated mostly with severe storms, have been investigated by means of geostationary meteorological satellites. Cold U-shaped and embedded warm spots, as well as cirrus cloud layers above the anvil in the lower stratosphere, have been observed by, among others, Fujita (1981, 1982), Negri (1982), Mack et al. (1983), and Heymsfield et al. (1991).

The geometric and spectral resolution of the Advanced Very High Resolution Radiometer (AVHRR) on board National Oceanic and Atmospheric Administration (NOAA) polar orbiters lends itself well to the detection of small-scale structures of storm tops not adequately evinced by geostationary satellite imagery. Liljas (1984) and Scorer (1986) first reported increased radiance in channel 3 (3.55–3.93 μm) on top of some convective storms, recognizing the channel's potential for the identification of inhomogeneities in their microphysical composition. Setvák and Doswell (1991) report observations of deep convective storms based on AVHRR's channels 2 (0.725–1.1 μm), 3, and 4 (10.3–11.3 μm). Observations of convective storms in NOAA/AVHRR imagery at the Czech Hydrometeorological Institute since 1984 have shown the existence of at least two major types of increased channel 3 cloud-top reflectivity (Setvák 1989): the ''convective cell-like'' and the much less frequent ''plume-like.'' The present paper focuses on the presence of ''plumes'' on top of some convective storms. These structures clearly appear against the anvil background in channel 2 or 3 and often in both. They originate from a very small spot (the size of a few pixels) in the storm's embedded warm area and spread downwind, resembling plumes from a chimney. Observations in channel 2 show in most cases the vertical separation between the plume and the underlying anvil. Observations of several storms in Europe and a discussion of their possible origin are reported.

2. Observations

Two observations of plume-producing storms are detailed as a basis for discussion. The reader is also directed to Setvák and Doswell's (1991) case of a mature supercell storm on 18 August 1986 1330 UTC over the Czech Republic. This storm shows all the typical satellite-observed features associated with supercell storms: cold U-shape (horseshoe), close-in and distant warm areas, and an extended anvil cloud.

a. Meteorological situation

Figure 1 shows a mature multicell storm on 6 July 1988 1348 UTC over southern Poland and north-central Slovakia as seen by *NOAA-9*. The surface chart at

Corresponding author address: Dr. Vincenzo Levizzani, Istituto FISBAT–CNR, via Gobetti 101, I-40129 Bologna, Italy.
E-mail: vince@rain.fisbat.bo.cnr.it

v4483 / ams v4304 1279 Mp 361 Friday Oct 11 01:35 PM AMS: J At Sci (February 1 96) 1279

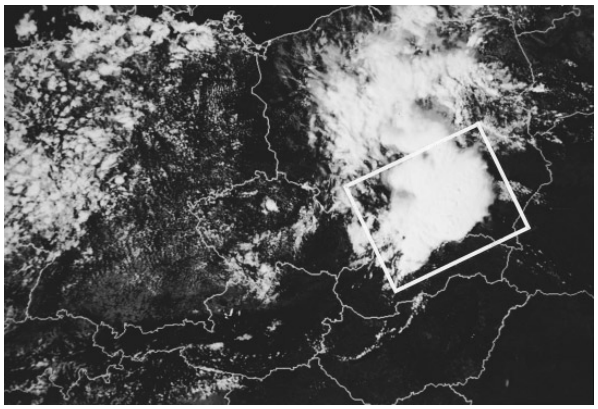

FIG. 1. 1348 UTC 6 July 1988: AVHRR *NOAA-9* channel 2 image of the multicellular storm over north-central Slovakia and southern Poland (1400 km × 1050 km). The box delimits the area covered by all the subsequent images of the storm.

1200 UTC of the same day (not included) exhibits a cold front that, encircling a moderately high pressure center (1020 hPa) over eastern Germany and the Czech Republic, extended from northeastern Italy across eastern Europe to the Baltic countries and then hooked around to southern Sweden and Norway. On the border between Poland and Slovakia, cumulus and cumulonimbus were reported with the formation of thunderstorms over a wide area; altocumulus were also observed from Russia down to Austria and Germany. The system was in the mature stage at the time of satellite observation, and at least two convective cores were active.

Figure 2 shows a multicell storm on 30 July 1994 0517 UTC over Normandy and the English Channel as seen by *NOAA-11* (biggest, elongated structure inland) accompanied by the convective cluster of a companion storm (offshore). The meteorological situation at 0000 UTC shows a depression over northwestern Europe, which constitutes a typical summer event when the polar front along the westerlies extends down to relatively low latitudes between 40° and 50°N. The system was driven by the wide low pressure area with its epicenter of 985 hPa immediately south of Iceland. Along its meridional border was a family of intensifying thunderstorms at various stages of development that was moving toward central Europe. This was more or less the case when the satellite passed over and documented a series of active convective centers, besides the one we are describing, over eastern France, Switzerland, Germany, Belgium, the Netherlands, and southern Denmark. Extensive precipitation was reported all over central and eastern Europe resulting from the convergence of warm air from the SW and cold unstable air from the NW. An analysis of Meteosat infrared (IR) images detects a first storm around 2300 UTC on 29 July just south of Normandy and another storm forming west of it at 2400 UTC. The storm cluster already included three storms by 0100 UTC on 30 July, and these grew considerably bigger along a convergence line stretching across Normandy to Brittany, where a new storm formed around 0200 UTC. Around the time of the NOAA passage, the storms were already massed together, and the multicell was growing at a steady pace, eventually acquiring the form of a supercell storm (note that no radar observations are available so that the inference of the multicell and supercell character is entirely from satellite observation, chiefly IR). While the storm west of it decayed around 0730 UTC, the multicell storm seemed to reach maturity at 0800 UTC and then proceeded in an ENE path to sweep first the French coast of the English Channel and then the southeastern United Kingdom. The system disappeared by 1200 UTC.

b. Near and thermal infrared

Significant cloud-top structures usually associated with supercell storms were first described by Fujita (1981) on the basis of IR imagery from the Geostationary Operational Environmental Satellites (GOES). A detailed overview of the observations of thunderstorm cloud-top surfaces can be found in, among others, Adler and Mack (1986), Heymsfield and Blackmer (1988), and Heymsfield et al. (1991).

AVHRR channel 2 near-infrared observations allow for a recognition of the spatial organization of the storm at very high resolution: cell positioning, anvil extent, wavelike patterns, and shadow casting. Although the plumelike features are primarily observed in channel 3 imagery, it is possible in some cases to resolve them simultaneously or detect them only in visible channel 1 (0.58–0.68 μm) or near-infrared channel 2. Thermal IR cloud-top maps reveal the arrangement of convective cores, close-in and distant warm areas, and, under certain circumstances, give an idea of the elevation map

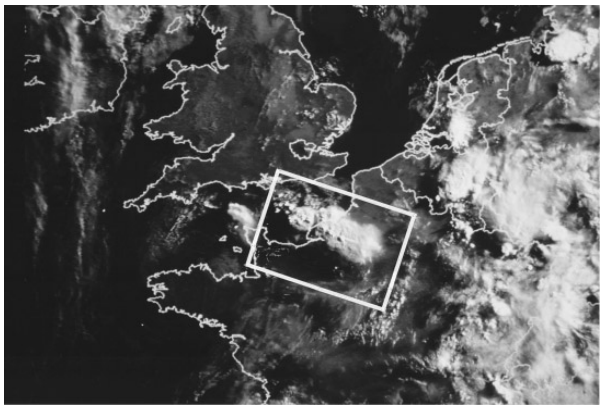

FIG. 2. 0517 UTC 30 July 1994: AVHRR *NOAA-11* channel 2 image of the multicellular storm over Normandy and the English Channel (1400 km × 1050 km). The box delimits the area covered by all the subsequent images of the storm.

of the top by means of combined radar and satellite stereoscopic and IR observations as done by Negri (1982) using GOES imagery.

A plume is detected in the channel 2 image of the 6 July 1988 storm (Fig. 3a), and its presence is evident also from channel 4 (Fig. 3b), which in our experience is very uncommon. The ''source'' of plumes is normally shifted downwind from the coldest areas, as it is for this storm (Fig. 3c). Here, given the very narrow width of the object at its very beginning in channel 2, it is located in a pointlike area (a few kilometers in diameter) within the warm spot of the big eastern cell. The shadows being cast by the plume on the surrounding anvil top indicate its vertical separation from the surrounding anvil, thus suggesting that the generating mechanism is other than the anvil-producing one. One more argument in favor of the separation, even though not conclusive, is that the structure of the plume is more or less preserved in channel 4, indicating a temperature difference between the particles of the plume and the surroundings. A vertical separation could well account for this difference. Naturally, a different channel 4 emissivity of the smaller particles forming the plume and the surrounding anvil is another candidate explanation.

The separation of the plume from the anvil top is much more evident from the 30 July 1994 storm. The height of the sun above the horizon is approximately 1.8 degrees, and the storm is situated at the center of the satellite pass so that the sensor is looking at it nearly from above. The very favorable sun–satellite–storm position in the early morning produced larger shadows in channel 2 (Fig. 4a), which show the plume body as emerging from the storm's main structure. Here, the plume is more like a ''split plume'' with two very bright splinters emerging from the source, which again is to be found in the warm spot of an active cell (see channel 4 image in Fig. 4b and diagram in Fig. 4c).

The two arms of the plume show up also in channel 4 as narrow discontinuities in the cloud-top thermal field. The ''stratospheric cirrus at the height of 15 km in the form of two fingers . . . in the area of the distant warm area'' on GOES visible (VIS) imagery reported by Mack et al. (1983) seems to be very similar to the split plume of the 30 July 1994 storm and to that of the storm in Setvák and Doswell's (1991) Fig. 4. The cy-

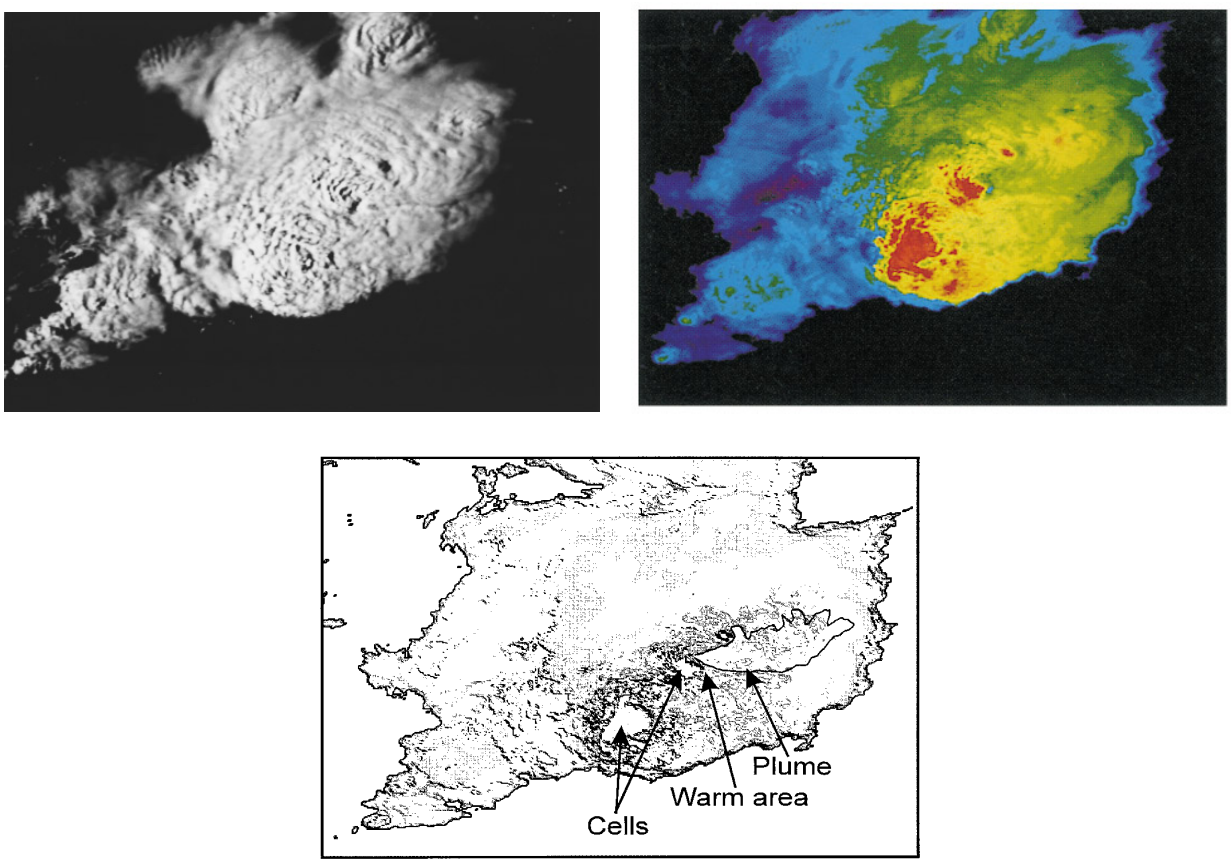

FIG. 3. 1348 UTC 6 July 1988: (a) Channel 2 image; (b) channel 4 image with temperature range between 205 (red) and 255 K (blue); (c) schematic diagram showing locations of cells, warm area of eastern cell, and plume (440 km × 330 km).

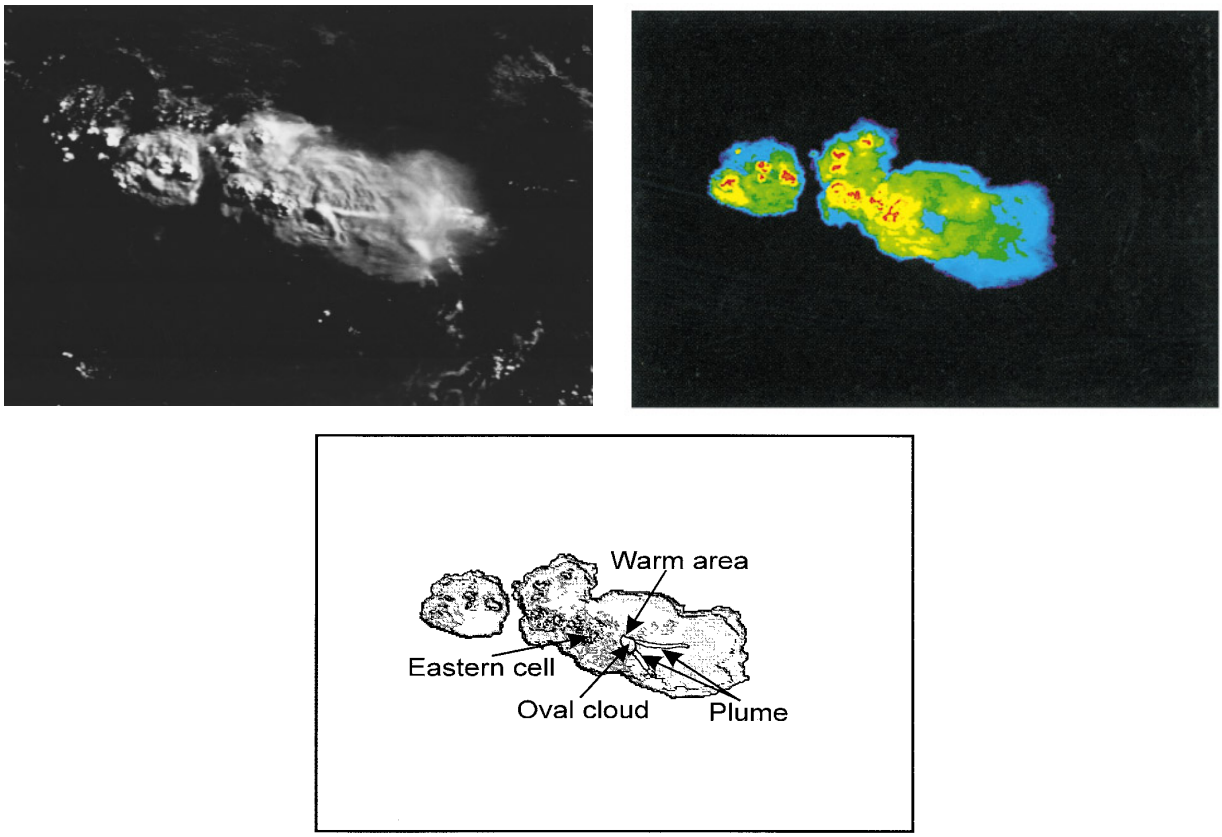

FIG. 4. 0517 UTC 30 July 1994: (a) Channel 2 image; (b) channel 4 image with temperature range between 208 (red) and 228 K (violet), a temperature of 204.5 K for the eastern overshooting top in the western storm (minimum temperature of the whole image), 208.5 K for the overshooting top closest to the plume source, and 220.5 K the highest temperature within the warm spot; (c) schematic diagram showing locations of eastern cell, its associated warm area, plume's arms, and oval cloud (440 km × 330 km).

clonic curvature of the northern branch and the anticyclonic one of the southern in the present case suggest that some kind of opposing rotations are responsible, together with the diverging cloud-top outflow, for the plume's forking. No inference whatsoever can be made about the nature of these rotations as they originated above the anvil or belonged to the ascending flow.

A bright spot in channel 2 in the form of an oval cloud is detected in the same position as the plume's source. The shadow cast by this rounded cloud appears much longer than that of the plume, suggesting that we are looking at separate objects, perhaps at two different heights. Very simple geometric computations based on the shadow width give a height of about 300 m above the anvil top for the oval cloud and a height of 50 m for the plume's north branch. No conclusions can be drawn as to whether the source for both the oval cloud and the plume is the same or not. An analysis of Meteosat imagery was carried out without success. Meteosat VIS images (0.5–0.9 μm) are available only from 0600 UTC: images at 0600 and 0630 UTC in single and double resolution showed no trace of the plume, nor did the IR Meteosat image at 0500 and 0530 UTC. The reason for this is most surely the fact that Meteosat spatial resolution is not high enough in the majority of cases to detect small-scale features at the cloud top.

c. *The 3.7-μm spectral band*

AVHRR channel 3 is located in the spectral region that includes both emitted and reflected components, being at the long wavelength end of the solar spectrum and at the short wavelength end of the blackbody emission spectrum at earth temperatures (Scorer 1986). The channel 3 cloud-top appearance exhibits a complex dependence on several parameters for both the thermal (temperature, emissivity, transparency) and reflected (reflectivity, transparency, solar zenith angle, geometrical parameters affecting backscattering) components. Many of these radiative properties are closely linked to cloud-top microphysics and are strictly interconnected (Hunt 1973; Scorer 1986). The channel is used for the detection of ice particles at cloud top since they are very absorbent at these wavelengths. Some convective storms feature areas of increased outgoing channel 3 radiance (Liljas 1984, 1986), which is to be ascribed

FIG. 5. 1348 UTC 6 July 1988: Channel 3 cloud-top reflectivity with values ranging from 0 to the 7.5% increase of the plume (440 km × 330 km).

to the reflected component (Setvák 1989). Therefore, the reflected component, specifically the channel 3 cloud-top reflectivity (Setvák and Doswell 1991), is to be further investigated for a satisfactory interpretation of the observed increased radiances.

The increased channel 3 cloud-top reflectivity is the primary way to identify these objects, whose shape clearly resembles a plume or a ''fan'' emanating from a relatively small spot (the source), whose size is of the order of a few pixel units (a few kilometers at most). Another important characteristic is that their length can stretch along the entire anvil and even beyond its margins without any significant intervening decrease in reflectivity; Setvák and Doswell (1991) have reported an example for a supercell storm (see their Fig. 4). The mechanism responsible for the production of such a plume's particles is necessarily a very stable one in order to give rise to plumes of the observed length. Given upper-level relative winds of the order of 10 to 25 m s^{-1}, the lifetime of the source is of the order of tens of minutes, perhaps even several hours.

The channel 3 cloud-top reflectivity image of the 6 July 1988 storm (Fig. 5) shows a strong increase in reflectivity over the object identified as a plume in channel 2 with a very sharp radiance gradient in the southern flank. The most important difference between the shape of the plume in channels 2 and 3 is at the source, where the very beginning is missing in channel 3 but clearly detectable in channel 2. It seems that the mechanism producing the plume, rather than ceasing sometimes, has here simply undergone a modification resulting in a different microphysical composition of the plume, as suggested by the decrease in channel 3 reflectivity. Note that the plume is not split into two beams, as is often the case, but has an intact body, which probably reflects the environmental conditions of the layer.

The plume of the 30 July 1994 storm is associated with only a slight increase in channel 3 reflectivity (Fig. 6). The increased reflectivity coincides with the two ''arms'' delimiting the area of the plume and already described for the channel 2 image. The oval cloud observed as a bright spot in channel 2 also exhibits increased channel 3 reflectivity, thus revealing a similar composition with respect to the plume, a fact that could not be proved by simple channel 2 and channel 4 analysis. Note, however, that due to the very low sun elevation angle, no exact quantitative estimate of channel 3 reflectivity can be performed in this case.

d. Multispectral analysis

The complexity of the described cloud-top phenomena associated with deep convective storms requires detailed multispectral analysis of AVHRR data in order to extract information that would otherwise remain concealed in single-channel analysis. The main goal is to associate features observed in individual channels and, consequently, to gain higher-order insights into a storm's cloud-top structure.

In most cases very accurate image processing reveals shadows cast by the plumes on the anvil cloud top. This proves that, on these occasions at least, the height of the plume tops is greater than that of the anvil cloud top. That shadows are not always detectable can be attributed to either unfavorable geometrical arrangements of the sun–satellite–cloud-top system or the characteristics of a particular plume (e.g., diffused edges, high transparency, or the plume being embedded in the anvil). When detected in channels 1 and 2, the plumes are partially transparent. These facts, that is, shadows and partial transparency, prove that plumes constitute an independent upper-level structure of these storms and therefore must be generated by mechanisms other than the anvil-producing one. These observations match Fujita's (1982) on low-stratospheric cirrus

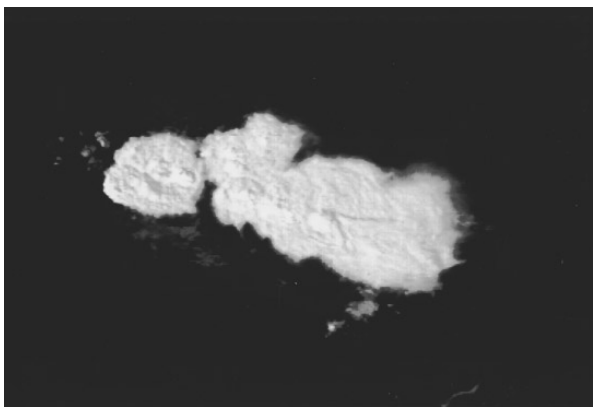

FIG. 6. 0517 UTC 30 July 1994: Original channel 3 image (no quantitative channel 3 cloud-top reflectivity analysis was performed due to very low sun elevation angle) (440 km × 330 km).

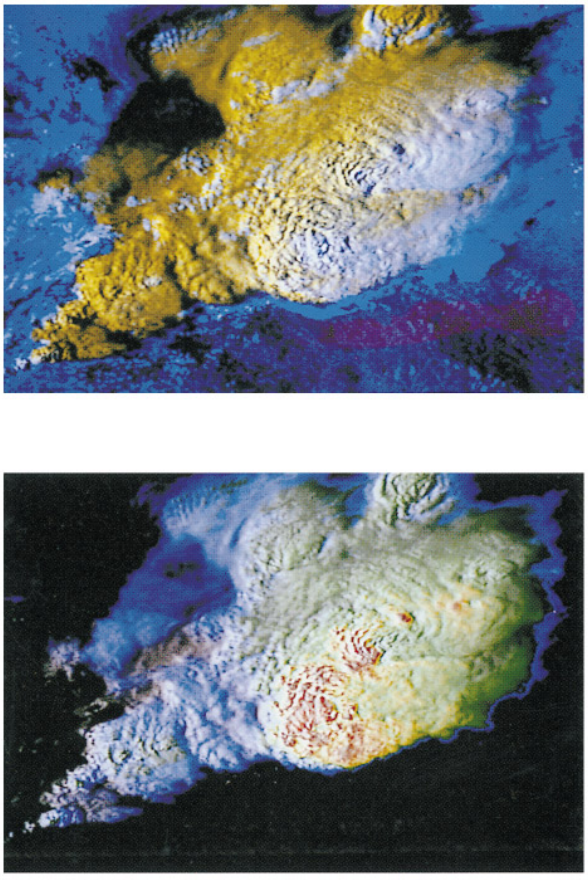

FIG. 7. 1348 UTC 6 July 1988: (a) Multispectral synthesis of channel 2 (yellow shades) and channel 3 cloud-top reflectivity (blue shades); (b) enhanced channel 2 obtained by superimposing channel 4 color palette as in Fig. 3b. The plume appears evident in the mid-eastern section of the storm in channels 2 and 3 and a little less so in channel 4. Its separation from the anvil top becomes more evident in the multispectral images (440 km × 330 km).

above the anvil and corroborate the cirrus's separation from the anvil's structure as depicted in Fujita's (1982) Fig. 11. The plumes are normally undetectable in channels 4 and 5 and only on some occasions, like those of the storms presented in this paper, do they increase the anvil cloud-top temperature by 1 or 2 K.

Multispectral, color composite syntheses of at least two channels into one image are commonly used in a wide range of remote sensing applications. The color of a particular object in such a composite image results from the ratio of basic colors (red, green, and blue in most cases) that are assigned to the individual spectral channels combining in the synthesis. This technique enables easier object recognition in the final image, as the resultant colors depend on the multispectral characteristics of the objects. In meteorology, such techniques are mainly applied to cloud classification for weather analysis and forecasting (e.g., Karlsson and Liljas 1990).

Channel 2 in Fig. 7a is associated with yellow shades, and channel 3 cloud-top reflectivity with blue ones. Relatively high channel 3 reflectivity of the plume in conjunction with high albedo and texture in channel 2 manifestly demonstrates that the plume is overshooting the anvil top by very clearly delimiting and giving depth to its southern flank. The channel 2 image of the same storm of 6 July 1988 is enhanced by superposition of the channel 4 temperature field in Fig. 7b: the result is the channel 2 structure colored with the palette of channel 4. This makes it possible unambiguously to observe that the plume's temperature is higher than the surrounding anvil's, thereby situating it higher up in the stratosphere. Moreover, the collocation of the plume's source in channel 2 and the warm spot in channel 4 are shown.

Channel 2 is associated with blue shades (the brighter the shade, the higher the channel 2 albedo), and channel 4 with red (the brighter the shade, the colder the cloud top) for the 30 July 1994 storm in Fig. 8. The bifurcation of the plume in two arms is enhanced, thus confirming that it is an object separated from the anvil body.

The very limited number of available cases documented by NOAA imagery stems from the relative rareness of plume-generating storms over Europe, so that their observations are very sparse. Twelve plume-producing storms have been examined heretofore: five had a cold U, and the plume originated from either a close-in or distant warm area; four did not show any U (or V), and the plume still emanated from a warm spot; and in the last three the plumes were not connected to any significant structure in channel 4, and their source was in the region downwind from the storm's core. The synthesis of channels 3 (blue) and 4 (red) of the 18 August 1986 storm [see Setvák and Doswell (1991) for single-channel imagery] in Fig. 9 clearly identifies the distant warm area as the source of the split plume.

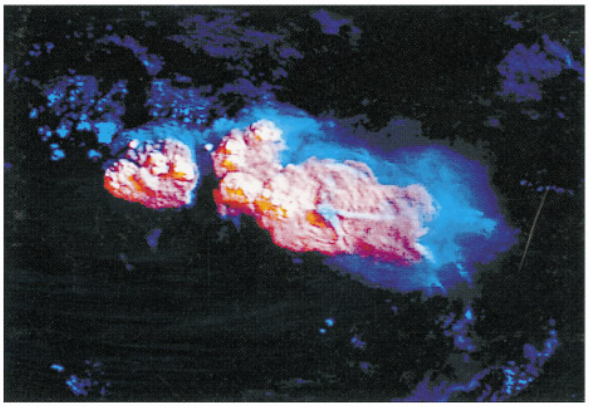

FIG. 8. 0517 UTC 30 July 1994: Multispectral synthesis of channels 2 (blue shades) and 4 (red shades) (440 km × 330 km).

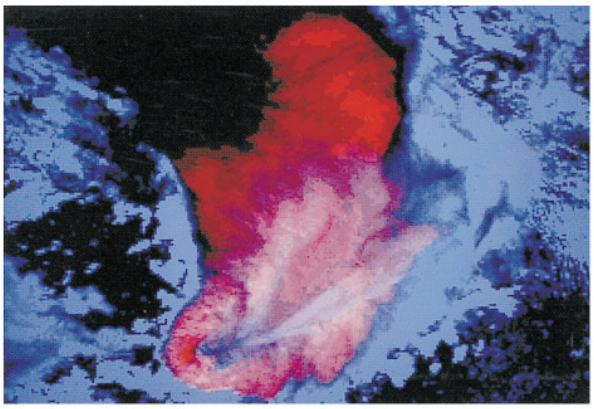

FIG. 9. 1330 UTC 18 August 1986: Supercell storm over north-central Bohemia. Synthesis of channel 3 cloud-top reflectivity (blue) and channel 4 (red). The multispectral image shows that the plume emanates from the channel 4 distant warm area [the reader is directed to Setvák and Doswell (1991) for single-channel imagery] (440 km × 330 km).

From an analysis of convective storms in which the well-pronounced warm–cold couplet appears simultaneously with channel 3 plumes, it follows that the plumes emanate from warm spots located within storm cores.

Synthesis of channel 2 and channel 4 data in some cases indicates that a dark spot in channel 2 not associated with any nearby overshooting top might be collocated with the channel 4 warm spot (emanating a plume visible in channel 3). This can either correspond to the presence of a cloud-top slope or turret (McKee and Klehr 1978) or a significantly lower ice particle concentration. However, the relative positioning of the sun–satellite–cloud-top system and the highly variable cloud-top topography, which markedly affect channels 1 and 2 data, usually make these images difficult to interpret unambiguously.

Plumelike features are occasionally detected in channel 1 or channel 2 imagery, with no correspondence in channel 3. It remains to be seen whether such events are at all related to the plumes in channel 3, differing simply as to particle size, shape, or orientation, or represent a completely different phenomenon, perhaps a wavelike disturbance.

3. Discussion

Very small ice particles, whose size is comparable or somewhat larger than channel 3 wavelength, are very likely to increase channel 3 cloud-top reflectivity significantly (Hunt 1973; Arking and Childs 1985). The observation of enhanced channel 3 reflectivity throughout a storm's anvil indicates that the ice particles responsible for the increase in reflectivity at the cloud top persist there without major changes for a long time.

While ice crystal sizes in cirrus clouds of nonconvective origin range between several tens and hundreds of microns (Pruppacher and Klett 1978), the observed increased channel 3 cloud-top reflectivity values in convective storm tops suggest the presence of ice particles whose size is to be gauged in units of microns (size of the order of channel 3 wavelength). There might be two alternative processes leading to these increased small ice particle concentrations. First, the growth time of ice particles might be strongly limited as a result of violent vertical transport by analogy with the bounded weak echo region in radar observations of strong updrafts (Burgess and Lemon 1990). Second, the vertical lifting and/or gravitational settling might well separate the smallest particles at the cloud top. These mechanisms are currently beyond our verification capabilities and require observations by other techniques (e.g., airborne radar, in situ microphysical measurements).

Within the cloud-top temperature range of deep convective storms, only ice particles can be expected at the storm's top (Detwiler et al. 1992), although no conclusive information from in situ measurements is available at present on very small particle distribution (<10-μm size) inside severe storm cloud tops (Heymsfield 1986; Detwiler et al. 1992). Straka (1989) reports a considerable concentration of small ice particles at the anvil level in the simulation of a slowly evolving multicell storm over northeastern Colorado by means of the Wisconsin dynamical/microphysical model. The particles that formed in and near the updraft core grew rapidly in size before being transported upward and exhausted into the anvil, although a large number of them still remained at this level. The simulation of the 2 August 1981 Cooperative Convective Precipitation Experiment (CCOPE) supercell storm by means of the same model (Johnson et al. 1993, 1994) produces ice particles of 4–5-μm diameter in the bounded weak echo region (P. K. Wang 1994, personal communication), in good agreement with the observation of 6-μm particles in the same volume.

Having noted the presence of cirrus 1–3 km above the anvil top in the lower stratosphere, whose temperature was then higher than that of the anvil cirrus, Fujita (1982) proposed the following mechanism. The radiance emitted by the anvil cloud top can be increased by the thin, warmer stratospheric cirrus layer, wherein particle concentrations are higher in the wake (referring to the storm-relative upper-level winds) of the overshooting top. The generation of the stratospheric cirrus [photograph in Fig. 11 of Fujita (1982)] was attributed to the perturbation caused by violent collapses of the overshooting tops into the wake region.

No satisfactory mechanism for plume production can be put forward on the basis of these observations alone. The following considerations based on current findings, however, may lead to further investigations for a better understanding of the phenomenon.

- Plume formation and development as part of anvil growth seems unlikely at the present state of knowl-

edge. The present paper's channel 2 observation of shadows cast by plumes on the anvil background indicates their mutual separation. Heymsfield's (1986) results on ice particle evolution in the anvil of a severe thunderstorm during CCOPE show that aggregation is an important mechanism for particle growth in the anvil, where conditions are favorable for aggregation even at temperatures much below −20°C. With aggregation, the maximum particle size increases along with distance downwind of the updraft core. In the case of plumes, however, the increased channel 3 reflectivity remains more or less constant at great distance from the plume's source. It is reasonable to assume that the mechanism of plume formation and development is other than the ones involved in the anvil cirrus production.

• The plumes described in the previous sections show characteristics that identify them as different from Fujita's (1982) lower-stratospheric cirrus. First, they cover a well-defined area of the anvil downwind region and never occupy the entire anvil area. Second, they do not jump back and cover the overshooting top, as Fujita's (1982) do. The last, and probably most important, characteristic is their very small source (a few pixels in diameter). Located far behind the overshooting top, which can hardly represent the location of repeated violent collapses of the air from the dome, it is too constant both in space and time.

• The mechanism of subsidence and adiabatic warming for the formation of the close-in warm area proposed by Heymsfield et al. (1983) provides no clues as to the plume's formation. Their hypothesis, however, that the airflow over the overshooting top would resemble that over a mountain with consequent subsidence and damped oscillations presents another inference. The formation of plumes as a wavelike phenomenon in the lee of the overshooting top seems unlikely due to both the temporal stability of the plumes and the absence of any oscillations that would be clearly visible given the AVHRR resolution, which is much greater than the GOES IRs of Heymsfield et al. (1983). In other cases we have observed wave clouds on top of convective storms in the wake of overshooting tops or gravity waves related to pulsating updrafts, but in none of these was an increased channel 3 reflectivity observed.

Plume development was observed in one case (27 September 1992, not shown) for 2 h on Meteosat VIS imagery. The plume and the warm spot originated, evolved, and disappeared almost simultaneously, thereby suggesting the presence of a dynamic link between the two phenomena. This fact, together with the close link between plume source position and warm spot location, suggests that the theory of warm spot formation must include a mechanism for plume production under certain circumstances. The rapid scan mode of recent GOES-I carrying a 3.9-μm channel (Menzel and Purdom 1994) will, it is hoped, provide more detailed and timely observations of this link.

Acknowledgments. David W. Martin, Eric A. Smith, and anonymous reviewers deserve special thanks for their invaluable suggestions, which greatly improved the paper. The study was funded by the Czech Ministry of the Environment, Agenzia Spaziale Italiana, Gruppo Nazionale per la Difesa dalle Catastrofi Idrogeologiche, and Piano Finalizzato Sistemi Informatici e Calcolo Parallelo. One of the authors (MS) was supported by the European Communities as part of the Community's Action for Cooperation in Science and Technology with Central and Eastern European Countries, under Contract ERB 3510PL920837.

REFERENCES

Adler, R. F., and R. A. Mack, 1986: Thunderstorm cloud top dynamics as inferred from satellite observations and a cloud top parcel model. *J. Atmos. Sci.,* **43,** 1945–1960.

Arking, A., and J. D. Childs, 1985: Retrieval of cloud cover parameters from multispectral satellite images. *J. Climate Appl. Meteor.,* **24,** 322–333.

Burgess, D. W., and L. R. Lemon, 1990: Severe thunderstorm detection by radar. *Radar in Meteorology,* D. Atlas, Ed., Amer. Meteor. Soc., 619–656.

Detwiler, A. G., P. L. Smith, and J. L. Stith, 1992: Observations of microphysical evolution in a High Plains thunderstorm. *Proc. 11th Int. Conf. on Clouds and Precipitation,* Vol. 1, Montreal, PQ, Canada, International Commission on Clouds and Precipitation and International Association of Meteorology and Atmospheric Physics, 260–263.

Fujita, T. T., 1981: Mesoscale aspects of convective storms. *Proc. IAMAP Symp. on Nowcasting: Mesoscale Observations and Short-Range Prediction,* Hamburg, Germany, European Space Agency, 3–10.

——, 1982: Principle of stereoscopic height computations and their applications to stratospheric cirrus over severe thunderstorms. *J. Meteor. Soc. Japan,* **60,** 355–368.

Heymsfield, A. J., 1986: Ice particle evolution in the anvil of a severe thunderstorm during CCOPE. *J. Atmos. Sci.,* **43,** 2463–2478.

Heymsfield, G. M., and R. H. Blackmer Jr., 1988: Satellite-observed characteristics of Midwest severe thunderstorm anvils. *Mon. Wea. Rev.,* **116,** 2200–2224.

——, R. H. Blackmer Jr., and S. Schotz, 1983: Upper-level structure of Oklahoma tornadic storms on 2 May 1979. I: Radar and satellite observations. *J. Atmos. Sci.,* **40,** 1741–1755.

——, R. Fulton, and J. D. Spinhirne, 1991: Aircraft overflight measurements of midwest severe storms: implications on geosynchronous satellite interpretations. *Mon. Wea. Rev.,* **119,** 436–456.

Hunt, G. E., 1973: Radiative properties of terrestrial clouds at visible and infra-red thermal window wavelengths. *Quart. J. Roy. Meteor. Soc.,* **99,** 346–369.

Johnson, D. E., P. K. Wang, and J. M. Straka, 1993: Numerical simulations of the 2 August 1981 CCOPE supercell storm with and without ice microphysics. *J. Appl. Meteor.,* **32,** 745–759.

——, ——, and ——, 1994: A study of microphysical processes in the 2 August 1981 CCOPE supercell storm. *Atmos. Res.,* **33,** 93–123.

Karlsson, K.-G., and E. Liljas, 1990: The SMHI model for cloud and precipitation analysis from multispectral AVHRR data. PROMIS Rep. 10, Swedish Meteorological and Hydrological Institute, Norrköping, Sweden, 74 pp.

Liljas, E., 1984: Processed satellite imageries for operational forecasting. Swedish Meteorological and Hydrological Institute, Norrköping, Sweden, 43 pp.

——, 1986: Use of the AVHRR 3.7 micrometer channel in multispectral cloud classification. PROMIS Rep. 2, Swedish Meteorological and Hydrological Institute, Norrköping, Sweden, 23 pp.

Mack, R. A., A. F. Hasler, and R. F. Adler, 1983: Thunderstorm cloud top observations using satellite stereoscopy. *Mon. Wea. Rev.*, **111,** 1949–1963.

McKee, T. B., and J. T. Klehr, 1978: Effects of cloud shape on scattered solar radiation. *Mon. Wea. Rev.*, **106,** 399–404.

Menzel, W. P., and J. F. W. Purdom, 1994: Introducing GOES-I: The first of a new generation of geostationary operational environmental satellites. *Bull. Amer. Meteor. Soc.*, **75,** 757–781.

Negri, A. J., 1982: Cloud-top structure of tornadic storms on 10 April 1979 from rapid scan and stereo satellite observations. *Bull. Amer. Meteor. Soc.*, **63,** 1151–1159.

Pruppacher, H. R., and J. D. Klett, 1978: *Microphysics of Clouds and Precipitation.* D. Reidel, 714 pp.

Scorer, R. S., 1986: *Cloud Investigation by Satellite.* Ellis Horwood Ltd., 314 pp.

Setvák, M., 1989: Convective storms—The AVHRR channel 3 cloud top reflectivity as a consequence of internal processes. *Proc. Fifth WMO Conf. on Weather Modification and Applied Cloud Physics,* Beijing, Peoples' Republic of China, World Meteor. Org., 109–112.

——, and C. A. Doswell III, 1991: The AVHRR channel 3 cloud top reflectivity of convective storms. *Mon. Wea. Rev.*, **119,** 841–847.

Straka, J. M., 1989: Hail growth in a highly glaciated central high plains multi-cellular hailstorm. Ph.D. dissertation, University of Wisconsin—Madison, 413 pp.